

# Stress Distribution Around Mechanized Longwall Face at Deep Mining in Quang Ninh Underground Coal Mine

BUI Manh Tung<sup>1,\*</sup>, LE Tien Dung<sup>1</sup>, VO Trong Hung<sup>1</sup>

<sup>1</sup> Hanoi University of Mining and Geology, 18 Vien street, Hanoi, Vietnam

Corresponding author: [buimanhtung@humg.edu.vn](mailto:buimanhtung@humg.edu.vn)

**Abstract.** Quang Ninh underground coal mines are currently in the phase of finishing up the mineral reserves located near the surface. Also, in this phase, a number of coal mines have opened and prepared new mine sites for the extraction of the reserves at greater depth. Several mines have mined at -350 m depth and are driving opening excavations at -500 m depth below sea level. The mining at greater depth faces many difficulties, such as a significant increase in support and excavation pressures. The longwall face pressure is mostly manifested in great magnitude that causes support overloaded and jumped and face spall/roof fall. This paper, based on the geological condition of the Seam 11 Ha Lam coal mine, uses the numerical program UDEC for studying the impact of mining depth on stress distribution around the longwall face. The results show that the deeper the mining is, the greater the plastic deformation zone is. The peak front abutment stress moves closer to the coal wall, mainly concentrating on the immediate roof and top coal. The top coal is greatly broken, and its bearing capacity is decreased. Some solutions to the stability of roof strata are proposed, and a proper working resistance of support is determined. Additionally, the paper suggests that the starting depth for deep mining in Quang Ninh underground coal mines should be -350 m below sea level.

**Keywords:** Stress distribution, Longwall face, Deep mining, Underground coal mine, Quang Ninh

## 1. Introduction

Deep mining is an inevitable trend for coal mining in the world. According to statistics, there are many countries that perform the coal extraction at -500 m below sea level, such as -514 m in Russia, -928 m in Germany, -610 m in Poland, and -1,024 m in China [1]. These countries have early implemented research on mining at greater depth. Cheng et al [2] used numerical model in combination with theoretical analysis and site observation to interpret the typical stress distribution in roof and floor strata; deformation and failure of coal wall; and typical stress redistribution when mining depth varies. The study found the relationship between face support and roof strata in the condition of competent roof and deep mining. Liu [3] and Bai et al [4], by using the numerical program UDEC 3.0, studied the caving, stress field distribution and roof strata displacement as well as the impact of depth and dip angle on roof rock stability. The results provided scientific evidence and solutions for control of surrounding rock and face support. For studying behaviour of mine pressure and ground control at deep mining, Du [5] and Bai et al [6] used theoretical and practical investigations to predict the mode of failure zone, method for determination of main roof convergence, and relationship between dynamic pressure and mining depth. The results showed that the rock behaviour at deep mining was not clear, the frequency of coal wall spall/roof fall increased as mining depth increased, and the surrounding rock failed significantly. Qi et al [7] analysed ground pressure in deep mining from which fundamental and technical framework for prevention of dynamic impact at different scales in China. At the same time, Li et al [8] found a change in stress distribution at seam floor using numerical model, physical model and site measurement. Recently, Zhang et al [9] studied the stress distribution and failure characteristics of deep inclined seam. They revealed that the vertical taper structure was formed by the roof, interconnection and maingate. Besides, Chen et al [10] investigated deep mining in existence of face fault [10]. Chaoru [11] used regression analysis for studying distribution of in-situ stress in deep underground coal mines. It was found that an increase in mining depth increased the effect of in-situ stress on surrounding rock deformation and failure. However, as the depth increased, the increasing rate of horizontal stress decreases. The ratio of maximum principal horizontal stress to vertical stress was founded in the range of 0.63-2.42. According to Pathegame et al [12], deep mining becomes a common practice in near future, and it is controlled by the understanding of rock mechanics and mining technologies.

It can be seen that in the world, theories and practices for deep mining have been interpreted to some extent through theoretical analysis and site observation. The distribution of stress at great depth, however, is preliminarily studied through mainly numerical modelling. Only several input parameters have been

studied; accordingly, it lacks fundamentals for development of stress distribution around longwall face at great depth. For geological conditions in Vietnam, Le et al [13] used numerical method to study coal mining under competent roof at Quang Hanh coal mine, Quang Ninh coal field. The results showed that the face was affected by overburden pressure more seriously. It caused more face instabilities, especially near two roadways. Nguyen et al [14] developed a numerical model for calculation of failure and subsidence caused by mining for Quang Ninh coal field. An other example can be seen in Le et al in which a safe mining height for extraction of coal under Red River delta was determined and some feasible opening solutions were proposed [1, 15]. In general, the above studies are preliminary and lack detailed investigation for mine design and ground control at great depth.

## 2. Geological condition of longwall face

The mechanised face belongs to Seam 11 Ha Lam coal mine and in depth from -150 m to -300 m below sea level. The rock units in the mine include conglomerate, sandstone, gritstone, claystone, coal-clay and coal seams. The rock strata alternate each other, resulting in relatively consistent stratigraphic sequence in local scale. The roof and floor rocks are mainly siltstone, claystone and sometime sandstone layers. The rocks are medium strong. Seam 11 is ranks as thick seam but inconsistent in the range of 0.97-29.75 m and an average dip angle of 5 degrees. The longwall dimension in dip and strike directions are 120 m and 430 m, respectively. The rock characteristics are shown in Tab. 1.

**Tab. 1.** Characteristics of roof and floor rocks.

Surrounding rock	Rock types	Thickness, m	Rock characteristics
Main roof	Conglomerate	16.72	Sandstone-interbedded siltstone, equal distribution, thickness of 16.72 m. Medium to hard roof.
	Siltstone	8.48	
Immediate roof	Sandstone	2.11	Sandstone in thickness of 5-25 m, average of 17 m. Weak to medium stable roof.
Immediate floor	Sandstone, claystone	4.18	Claystone and coal-clay in lens shape of thickness 0.23-1.8 m. Sandstone in equal distribution in thickness of 2-15 m. Floor in stable to medium strong.
Main floor	Conglomerate	5.6	Siltstone-interbedded conglomerate, consistent distribution

## 3. Stress distribution around longwall top coal caving face in Quang Ninh

### 3.1 Model development

To study the stress distribution around longwall top coal caving face, this paper uses the numerical program UDEC 3.0 for modelling of longwall face [16]. Based on the geological condition of Seam 11, Ha Lam coal mine, the model has a length of 400 m, height of 126 m, depths of 300 m, 350 m, 400 m and 450 m. The block size is each stratum follows the status in practice.

The top boundary is applied a boundary stress in equal distribution. The bottom boundary is fixed with x- and y-velocity of zero. The side boundaries are fixed in horizontal displacement.

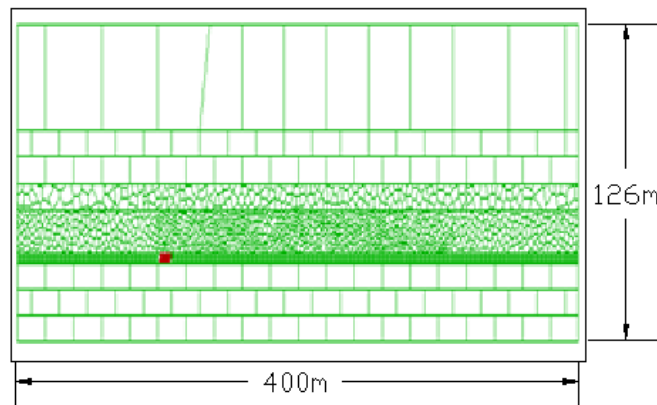


**Fig. 1.** Initial model.

### 3.2 Rock strata and coal seam properties

The rock behaviour in model follows Mohr-Coulomb theory. This theory can deal with fundamental rock problems such as slope stability and mining excavation. In coal mining, the theory can capture the failure, rupture and fault, and thus its parameters are of importance for calculation results. From the laboratory test, field observation and modelling experience from past users, the properties are chosen as follows:

**Tab. 2.** Rock and coal mechanical properties.

Rock strata	Density kg/m <sup>3</sup>	Uniaxial compressive Strength, MPa	Young modulus, GPa	Cohesion, Mpa	Internal friction, degree	Tensile strength, MPa
Upper main roof	2500	12	18	4	35	2
Lower main roof	2500	12	10	2	33	1.3
Immediate roof	2200	10	3	1.4	32	0.93
Coal	1400	3.2	1.2	1	33	0.3
Immediate floor	2679	12	3	1.4	35.8	0.93

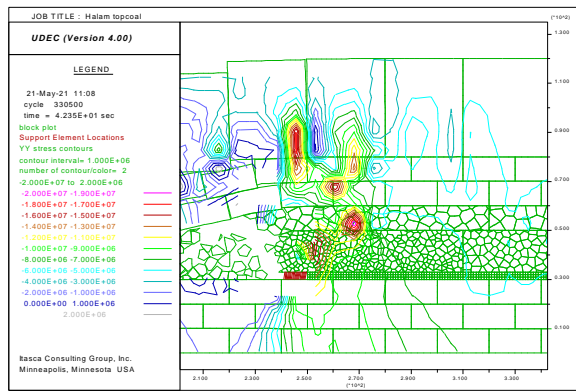
**Tab. 3.** Interfaces mechanical properties.

Rock strata	Normal stiffness, GPa/m	Shear stiffness, jGPa/m	Cohesion, MPa	Internal friction angle, degree	Tensile strength, MPa
Upper main roof	10	7	0.08	35	0.05
Lower main roof	9	6	0.06	32	0.04
Immediate roof	7	4.5	0	0	0
Coal	5	3	0.04	15	0.02
Immediate floor	7	4.5	0.04	15	0.04

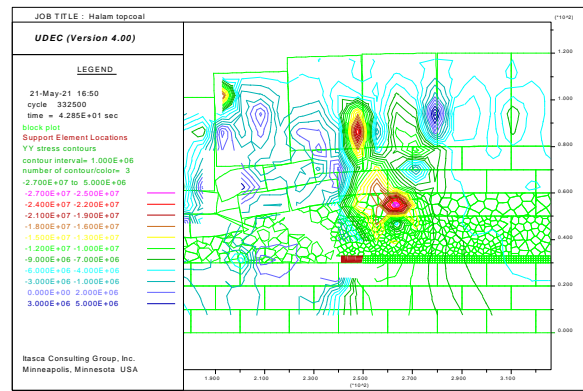
### 3.3 Front abutment stress distribution in variation of mining depth

Because the top coal fails under roof pressure, the front abutment stress forms distressed zone, concentrated zone, and pre-mining stress zone. Fig. 2 shows the stress distribution around longwall face when the mining depth is 300 m, 350 m, 400 m and 450 m. When the depth increases, the stress contour of front abutment stress varies. When the depth is 300 m, the concentrated front abutment stress zone locates at immediate roof and about 18 m ahead of coal wall with a peak stress magnitude of 20 MPa. When the depth is 350 m, the concentrated stress zone locates at immediate roof, about 15 m ahead of coal wall with a peak stress value of 27 MPa. When the depth is 400 m, the concentrated stress zone locates below immediate roof. The zone is about 13 m ahead of coal wall with a peak lue of 22 MPa.

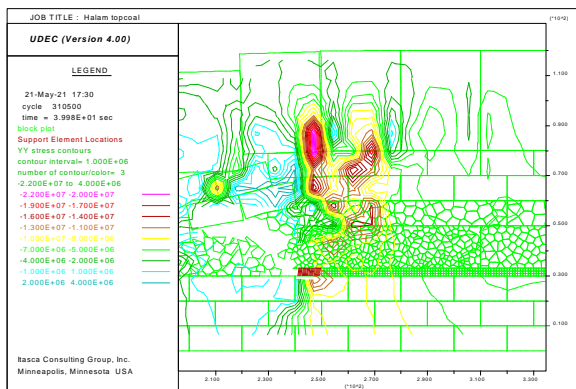
When the depth is 450 m, the zone locates at top coal section, about 8 m height compared to face floor and it has a peak stress value of 26 MPa. The numerical results indicate that when the mining depth increases, top coal fails significantly and the bearing capacity of top coal and immediate roof decreases. The concentrated stress zone moves closer to coal wall that in turns facilitates the failure of top coal. This however causes difficulty in face pressure control and support.



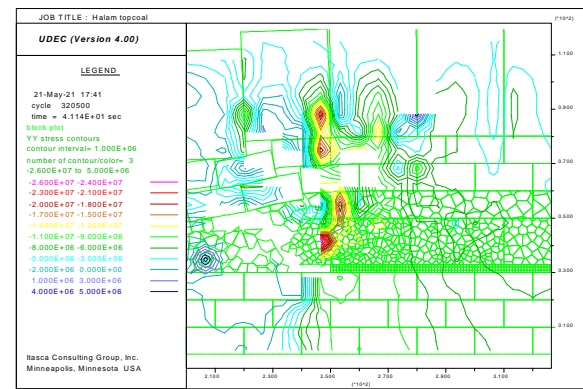
(a) Mining depth of 300 m



(b) Mining depth of 350 m



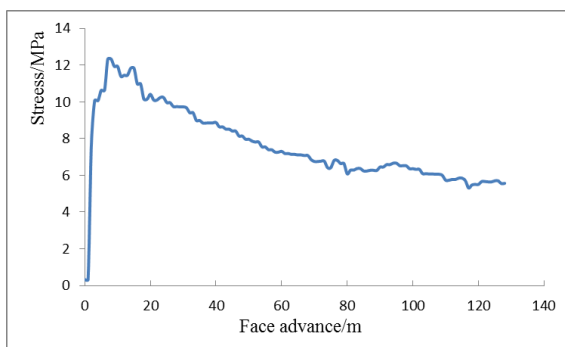
(c) Mining depth of 400 m



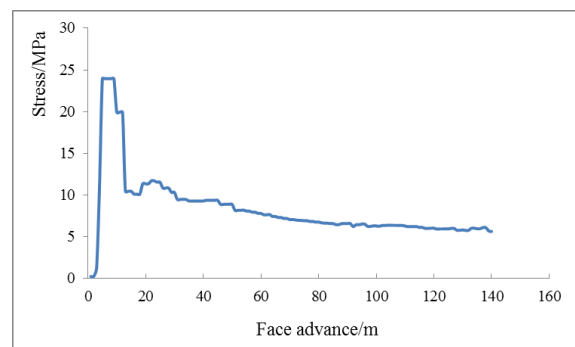
(d) Mining depth of 450 m

**Fig. 2.** Stress distribution in vertical direction in variation of mining depth.

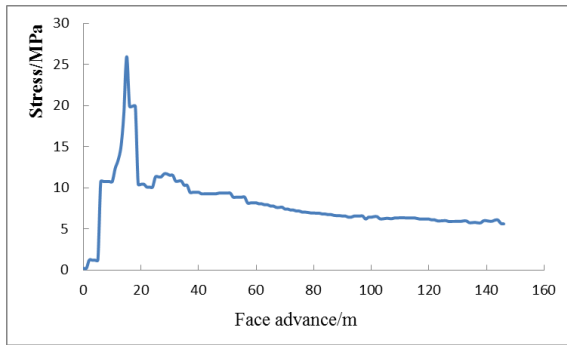
To interpret the stress distribution ahead of coal wall, a monitoring line was placed in top coal section and ahead of coal wall. The stress value measured along the monitoring line is shown in Fig. 3:



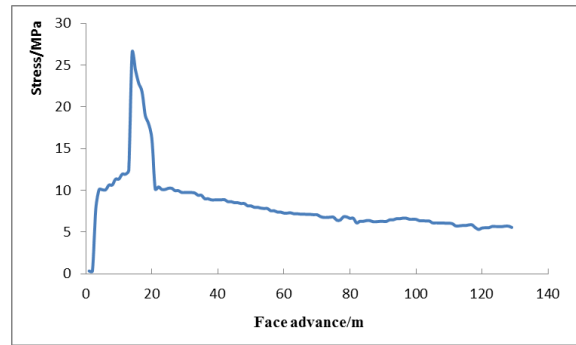
(a) Mining depth of 300 m



(b) Mining depth of 350 m



(c) Mining depth of 400 m



(d) Mining depth of 450 m

**Fig. 3.** Stress distribution along monitoring line in variation of mining depth.

Following the face movement, as the mining depth increases from 300 m to 350 m, 400 and 450 m, the location and magnitude of peak front abutment stress are 7.2 m, 5.2 m, 11.9 m, 12.1 m and 12.3 MPa, 23.95 MPa, 25.9 MPA, 26.5 MPa, respectively. The location and magnitude of peak front abutment stress are illustrated in Figs. 4-5.

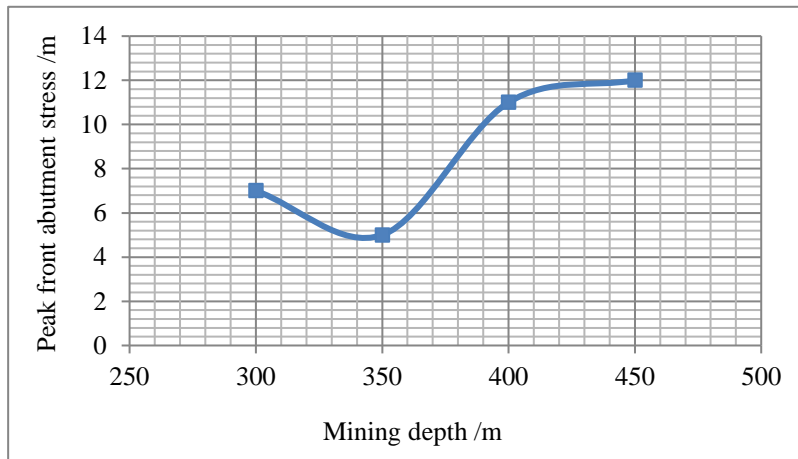


**Fig. 4.** Location of peak front abutment stress.

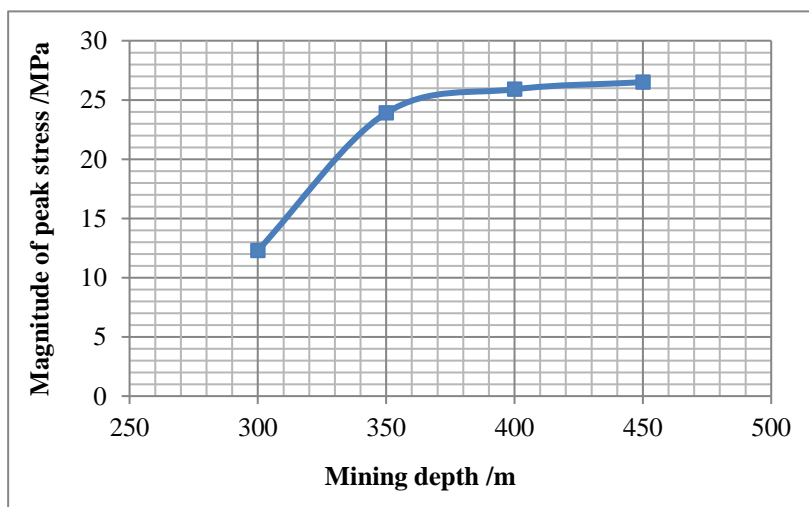


**Fig. 5.** Magnitude of peak front abutment stress.

Figs. 4 and 5 show that when mining depth increases, the location of peak abutment stress fluctuates. From 300 m to 350 m depth, it decreases from 7.2 m to 5.2 m. However, when the depth increases from

350 m to 450 m, the peak stress' location follows an increasing trend, from 5.2 m to 11.9 m. At the same time, the magnitude of peak front abutment stress follows a clear increasing trend. From the depth of 300 m to 350 m, the stress' magnitude increases significantly, from 12.3 MPa to 23.9 MPa. From 350 m to 450 m, the magnitude increases slightly. The modelling results clear reveal that when the mining depth increases, the peak front abutment stress increases. The decreasing rate of front abutment stress behind the peak point also increases. This study suggests a boundary for separating the shallow and deep mining portion of -350 m for Quang Ninh coal field.

### 3.4 Distribution of plastic deformation zone around longwall in variation of mining depth

Fig. 6 displays the degree of intact coal failure around longwall face. The top coal and immediate roof fail due to the rotational and shear effect from ruptured main roof and roof pressure from intact main roof. An increase in mining depth affects the stability of coal wall and extent of coal deformation ahead coal wall.

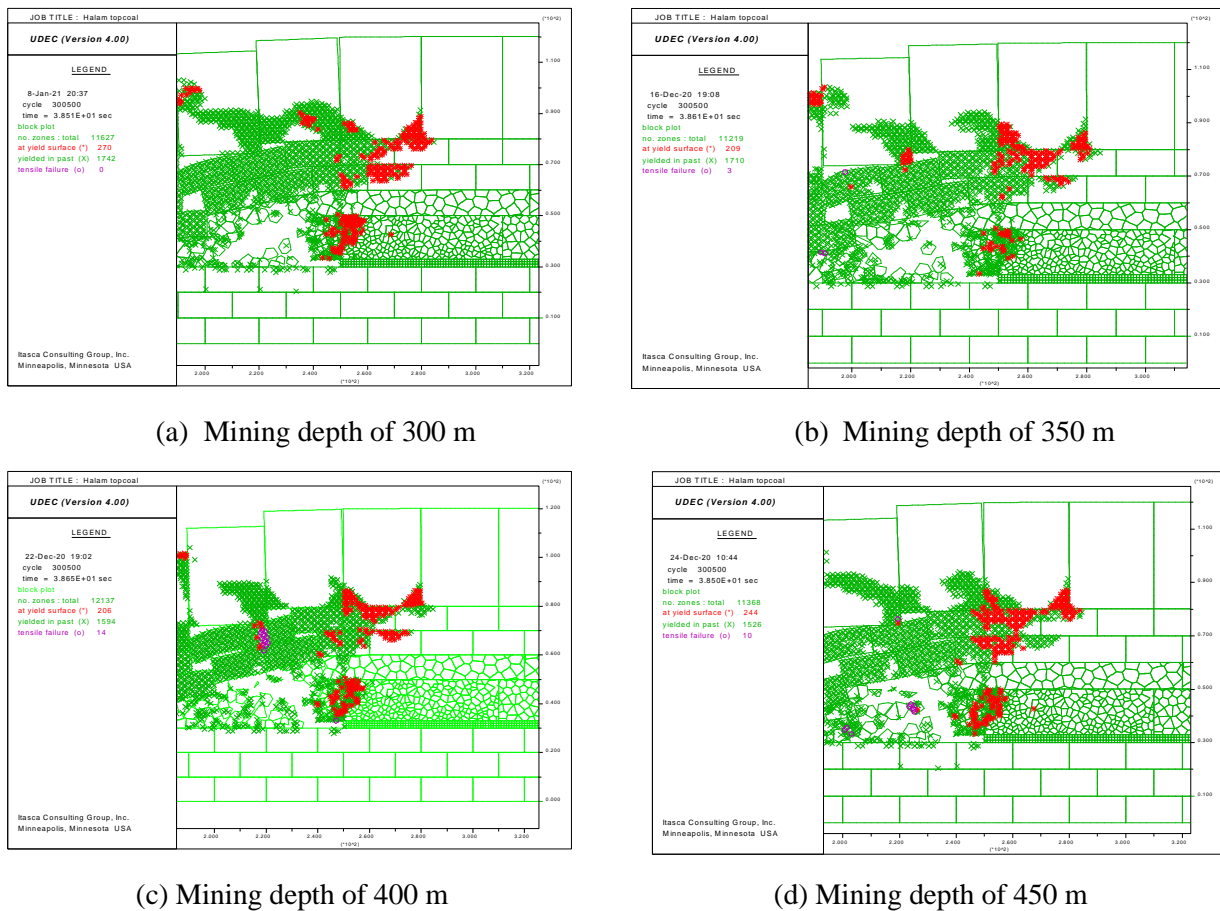


Fig. 6. Distribution law of deformation zone ahead of coal wall.

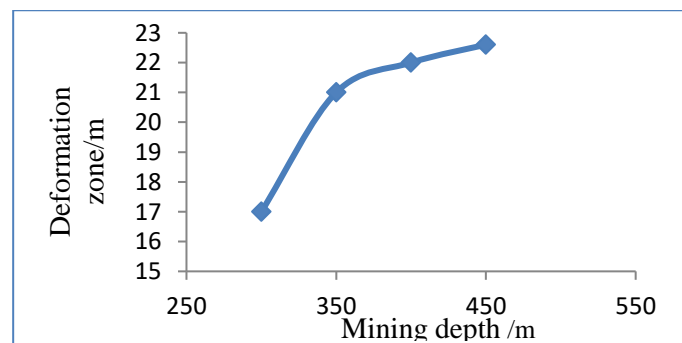


Fig. 7. Distribution of plastic deformation zone ahead of coal wall.

Fig. 7 displays the extent of plastic deformation zone in variation of mining depth. When the depth is 300 m, 350 m, 400 m and 450 m, the extent is 17 m, 21 m, 22 m and 22.6 m, respectively. The figure shows that when the depth ranges within 300-350 m, the deformation zone extent increases significantly by a value of 4.0 m, with an increasing rate of 0.08 m/m. When the depth increases from 350 m to 400 m, the zone extent increases slightly by a value of 0.5 m with a rate of 0.01 m/m. The extent increases greater in the depth range of 400-450 m with a value of 1.6 m and a rate of 0.032 m/m. Therefore, an increase in mining depth increases the extent of deformation zone as well, but with different rate.

#### 4. Distribution of load on face support

Seam 11 Ha Lam coal mine uses support ZF4400/16/28 along panel width and support ZFG4800/18/28 near two roadways. The profiles of immediate support load along panel strike and along panel width in the period of 11/3/2019–28/3/2019 are analysed. The data was collected from the real face.

##### 4.1 Distribution of support load along panel strike

Figs. 8-10 displays the profile of load distribution on support number 85, 15 and 55 along panel strike. The origin (0,0) is 50 m far away from the face entry, meaning that the main roof only collapses due to the mining cycle.

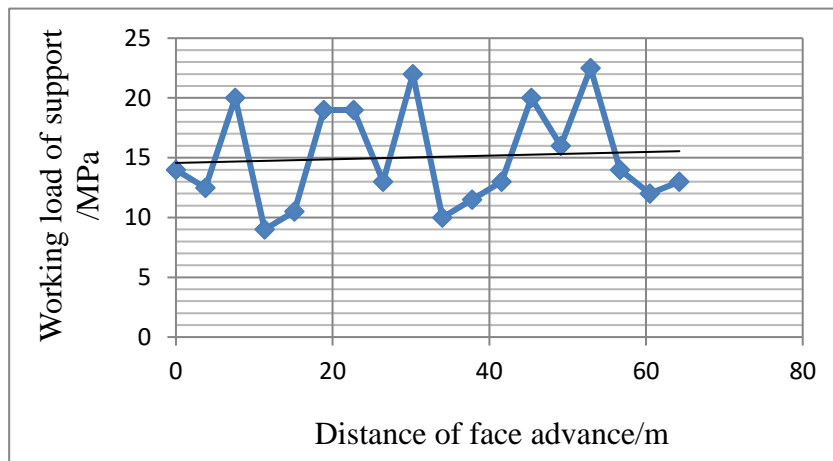


Fig. 8. Load distribution on support No. 85.

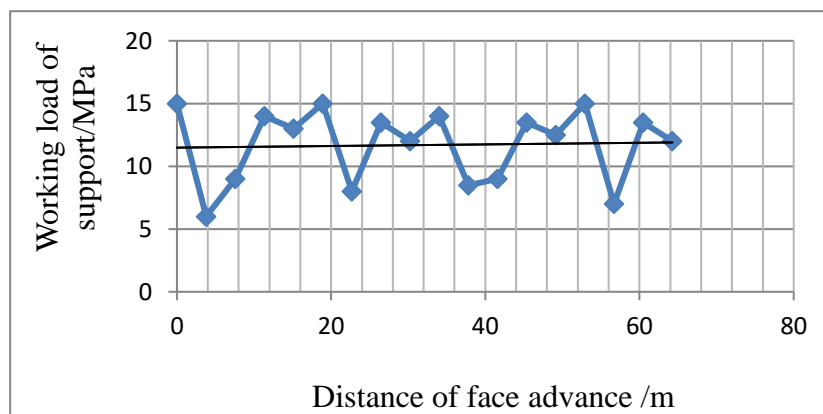
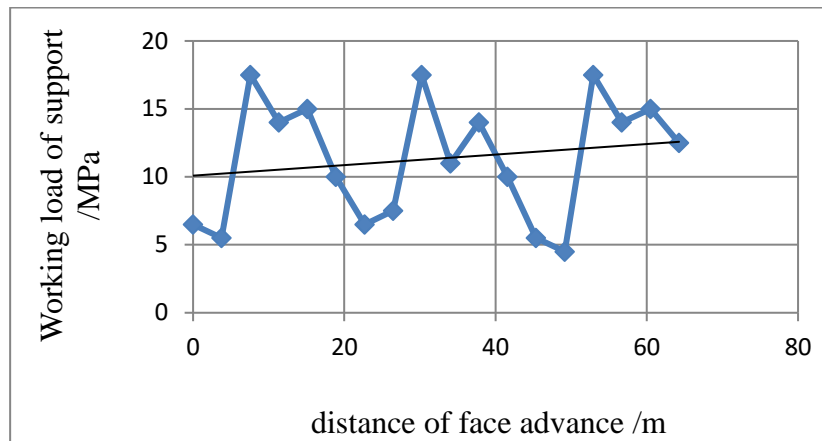


Fig. 9. Load distribution on support No. 15.



**Fig. 10.** Load distribution on support No. 55.

The three figures show that for the support No. 85 which is near tailgate, the maximum support load reaches 22.5 MPa with an average of 15.9 MPa. For the support No. 15 near maingate, the maximum support load reaches 15.5 MPa with an average of 12.3 MPa. For the support No. 55 at mid-panel width, the maximum load reaches 17.5 MPa with an average of 12.1 MPa. Therefore, the support load along panel strike follows a cyclically fluctuation. The distance between maximum points also varies in the range of 15-25 m. The result is consistent with the theoretical calculation of main roof fall in the design, which is 20 m [17].

In general, the roof structure in longwall top coal caving face after failure are also in beam form. The load on face support is smaller when the immediate roof ruptures before the rupture of main roof. This load is greater when immediate roof and main roof rupture at the same time. Thus, it is seen that the load support fluctuates cyclically with different values. In comparison with support capacity, the on-site support are totally capable of supporting the roof.

#### 4.2 Distribution of support load along panel width

The distribution of roof load on face support along panel width is shown in Fig. 11. This load distributes unevenly along the dip direction. At about 25 m near maingate and tailgate, the support load is greater than that in the interval between the two locations. Furthermore, the load on front leg pressure is commonly greater than that in rear leg, as shown in Fig. 11.

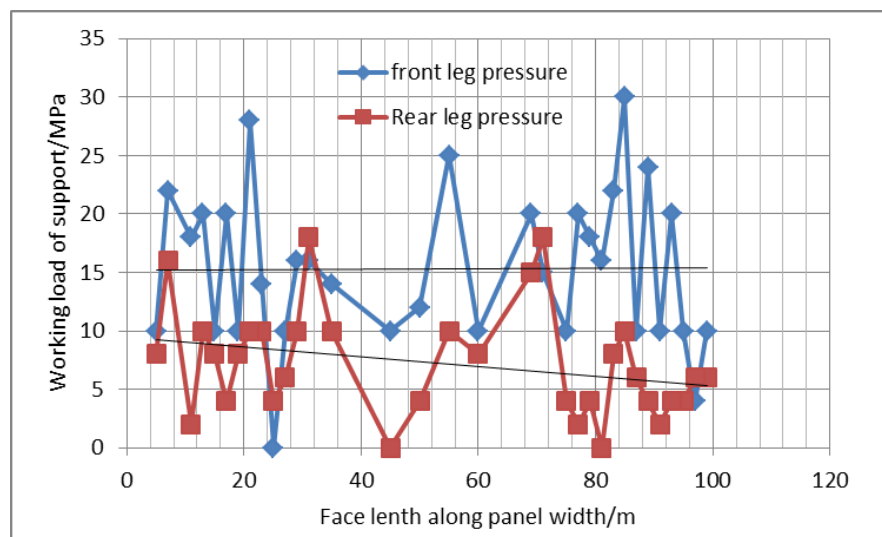


**Fig. 11.** Distribution of load on support along panel width.

The load distributions of front and rear legs show the difference. The maximum working load of front leg reaches 30 MPa with an average of 16.8 MPa. The maximum working load of rear leg reaches 18 MPa with an average of 8.56 MPa. However, at both face ends, the load is sometimes zero due to the breakage of safety valve as reported by on-site engineers. This also demonstrates the great magnitude of face roof pressure near two roadways.

## 5. Conclusions

1) When mining depth increases, the location of concentrated stress zone moves closer to coal wall, mainly distributed in immediate roof and top coal. The bearing capacity of top coal and immediate roof significantly decreases. An increase in mining depth therefore facilitates the failure of top coal while it causes difficulty for support and ground control.

2) The magnitude of peak front abutment stress varies clearly in variation of mining depth. When the depth increases from 300 m to 350 m, the stress increases rapidly with high rate, from 12.3 MPa to 23.9 MPa. The stress afterwards increases slightly when the depth increases to -450 m. Accordingly, this study proposes a boundary for separating shallow and deep mining portion of -350 m for Quang Ninh coal field.

3) When mining depth falls in the range of 300-350 m, the plastic deformation zone extends rapidly with a rate of 0.08 m/m. When the depth falls in the range of 350-400 m, the zone extends slightly with a rate of 0.01 m/m. The deformation zone extends greatly again with a rate of 0.032 m/m when the depth increases from 400 m to 450 m. It is concluded that an increase in mining depth causes an increase in extent of deformation zone as well but with different rate.

4) The working load on face support along panel strike changes periodically with an interval of 15-25 m. The load is also not consistent along panel width. It is commonly greater near T-junctions and smaller in the interval between the two junctions. The study confirms that the on-site face support totally meets the requirement of roof control.

## 6. Acknowledgements

The paper was presented during the 6th VIET - POL International Conference on Scientific-Research Cooperation between Vietnam and Poland, 10-14.11.2021, HUMG, Hanoi, Vietnam.

## 7. References

1. Le, N.H., Pham, T.H., Nguyen, C.K., Dao, T.C., 2011. Study on the influences during exploring deeper coal mines. 22nd National Conference on Mining Science and Technology. 323-327. (Vietnamese).
2. ChengJia, G., 2004. Characteristics of surrounding rock and support design procedures in working faces of strong roof and high ground pressure in deep mines. Master of philosophy, Shandong University of Science and Technology.
3. Liu, C.Y., Qu, Q.D., Wan, Z., 2002. Numerical simulation on rock stability in fully mechanized coal face under the condition of deep mining and large inclination. Chinese journal of rock mechanics and engineering, June 2002.
4. Bai, Q-S., Tu, S-H., Wang, F-T., Zhang, X-G., Yuan, Y., 2014. Observation and Numerical Analysis of the Scope of Fractured Zones Around Gateroads Under Longwall Influence. Rock Mechanics and Rock Engineering, 47, 1939-1950.
5. Du, J.P., Zhang, X.C., Jia, W., Yong, S., Chun, J., 2016. Characteristics of Strata Behaviors and roof control for longwall faces in deep mining. Journal of China university of mining & technology, 29(1).

6. Bai, Q-S., Tu, S-H., Chen, M., Zhang, C., 2016. Numerical modeling of coal wall spall in a longwall face. *International Journal of Rock Mechanics and Mining Sciences*, 88, 242-253.
7. Qi Q., Pan, Y., Shu, L., Li, H., Jiang, D.Y., Zhao, S., Zou, Y., Pan, J., Wang, K., Li, H., 2018. Theory and technical framework of prevention and control with different sources in multi-scales for coal-rock dynamic disasters in deep mining of coal mines. *Journal of China Coal Society*, 43(07). DOI: 10.13225/j.cnki.jccs.2018.0660-en.
8. Li, J.Z., Xie, Q.X., Wang, L., 2018. Failure Characteristics Induced by Unloading Disturbance and Corresponding Mechanical Mechanism of the Coal Seam Floor in Deep Mining, Preprints, engineering 2018, doi: 10.20944/preprints201804.0207.v1.
9. FengDa, Z., BaoHong, S., WenYan, G., 2020. Stress distribution and failure characteristics of deep inclined seam and overhead mining along strike longwall floor. *International Journal of Mining and Mineral Engineering*, Jan 2020, 11(4):306-322. <https://doi.org/10.1504/IJMME.2020.111933>.
10. Chen, X.H., Li, W.Q., Yan, X., 2011. Analysis on rock burst danger when fully-mechanized caving coal face passed fault with deep mining. *Safety Science*, 50(4): 645-648. <https://doi.org/10.1016/j.ssci.2011.08.063>.
11. Chao ru, L., 2011. Distribution laws of in-situ stress in deep underground coal mines, *Procedia Engineering* 26, 909 - 917, doi:10.1016/j.proeng.2011.11.2255.
12. Pathegama, G.R., Jian, Z., Minghe, J., Radhika, V.S.D., Tharaka, D.R., Adheesha, K.M., Bandara, S., 2017. Opportunities and Challenges in Deep Mining: A Brief Review , *Engineering*, 3, 546–551 , <http://dx.doi.org/10.1016/J.ENG.2017.04.024> .
13. Le, Q.P., Zubov, V.P., Dao, V.C., Vu, T.T.D., 2018. The rules apparition mine pressure and transfigure stone roof in the longwall mechanized furnace TT7.9–area Nga Hai, Quang Hanh coal company, Conference on earth sciences and natural resources for sustainable development (ERSD 2018). 224-229 (in Vietnamese).
14. Nguyen, Q.P., Pham, V.C., 2013. Investigation on development of geomechanical models for collaps and subsidence pridiction in underground coal mining in region Quang Ninh, *Journal of Mining and Earth Sciences*, 43, 64-71 (in Vietnamese).
15. Le, N.H., Nguyen, V.T., Bui, M.T., 2011. Determination of the safe mining depth when exploiting the Red River delta coal basin with underground coal mining and coal gasification methods. 22nd National Conference on Mining Science and Technology. 327-331. (Vietnamese).
16. Itasca Consulting Group, Universal Distinct Element Code (UDEC, FLAC, PFC) Verification Problems and Example Applications, Minneapolis, Minnesota, USA, 2000.
17. Le, T.D., Bui, M.T., Pham, D.H., Vu, T.T. & Dao, V.C., 2018. A modelling technique for top coal fall ahead of face support in mechanised longwall using Discrete Element Method. *Journal of Mining and Earth Sciences*, 59, 56-65.